Tissue Tracking: Applications for Brain MRI Classification

John Melonakos[a] and Yi Gao[a] and Allen Tannenbaum[a]

[a]Georgia Institute of Technology, 414 Ferst Dr, Atlanta, GA, USA;

ABSTRACT

Bayesian classification methods have been extensively used in a variety of image processing applications, including medical image analysis. The basic procedure is to combine data-driven knowledge in the likelihood terms with clinical knowledge in the prior terms to classify an image into a pre-determined number of classes. In many applications, it is difficult to construct meaningful priors and, hence, homogeneous priors are assumed. In this paper, we show how expectation-maximization weights and neighboring posterior probabilities may be combined to make intuitive use of the Bayesian priors. Drawing upon insights from computer vision tracking algorithms, we cast the problem in a *tissue tracking* framework. We show results of our algorithm on the classification of gray and white matter along with surrounding cerebral spinal fluid in brain MRI scans. We show results of our algorithm on 20 brain MRI datasets along with validation against expert manual segmentations.

Keywords: Bayesian Classification, Expectation-Maximization, Brain MRI, Image Segmentation

1. INTRODUCTION

Bayesian classification methods have been extensively used in a variety of image processing applications, including medical image analysis. The basic procedure is to combine data-driven knowledge in the likelihood terms with clinical knowledge in the prior terms to classify an image into a pre-determined number of classes. There is an extensive body of work which examines classification in this context using brain atlases and other spatial and shape priors on the medical image data.[1–3] Frequently, however, algorithms are required to perform in the absence of sufficient prior clinical knowledge and researchers revert to maximum-likelihood estimation which assumes uniform priors on the data.

In Figure 1, a categorization is portrayed which depicts a grouping of classification strategies which operate in the absence of clinical prior information. On the left, we show our algorithm which makes use of the prior terms by casting the classification problem in a slice-by-slice iterative framework. In the middle, we show our algorithm with uniform priors in a volumetric non-iterative framework. On the right, we group all other 3D classification algorithms which use uniform priors.

In this paper, we explore the use of minimal prior information. Simply stated, we wish to make use of the prior terms by incorporating useful information which can be entirely derived from the image header and data itself. The prior information we propose to use includes a combination of expectation-maximization weights and neighboring posterior probabilities. This will be described in greater detail in Section 2.3.

Before introducing our tissue tracking algorithm, we will discuss other Bayesian classification algorithms in Section 2.1 and 2.2. Second, in Section 2.3, we will outline our tissue tracking algorithm. Third, in Section 3, we will outline our experiments on 20 brain MRI data-sets. And, finally, in Section 4, we will present our results.

2. BAYESIAN CLASSIFICATION ALGORITHMS

In the first two subsections, we present previous work on Bayesian classification algorithms. First, we present work by Haker *et al.*[4] which outlines the general structure of Bayesian classification for tracking applications. Next, we present similar work by other groups which has been adapted for volumetric medical image segmentation. Then, in the last subsection, we present our work which casts the medical image segmentation into a tracking framework.

Further author information: (Send correspondence to J.M.)
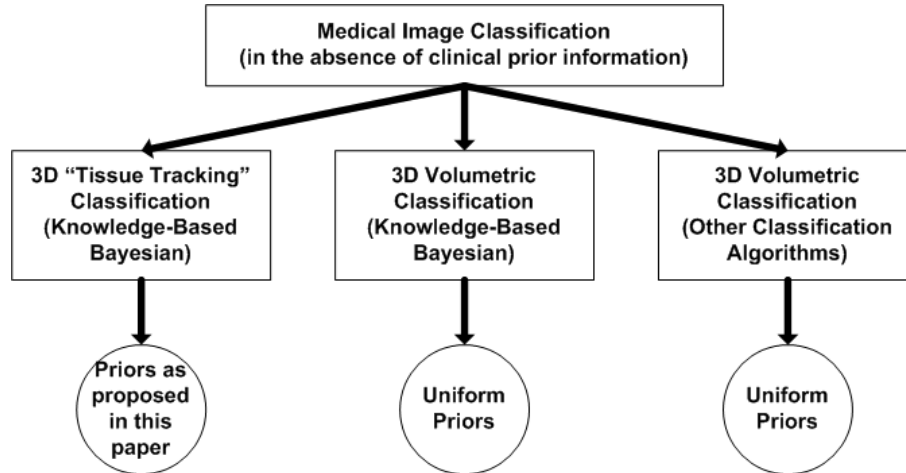J.M.: E-mail: jmelonak@ece.gatech.edu, Telephone: 1 678 229 6537

Figure 1. Medical Image Classification Strategies

2.1. 2D Tracking Algorithms

Several groups have previously proposed Bayesian classification algorithms. Most relevant to our work is the work by Haker *et al.* on the tracking of objects in 2D time-lapsed sequences of Synthetic Aperture Radar (SAR) data.[4]

At each time step in the tracking framework, the algorithm classifies the given 2D image slice into N classes. The segmentation proceeds as follows:

First, the image data is used to generate likelihood probabilities, $p(V|C)$, for a class C and an intensity value V. Typically, a normal distribution is assumed on the data and the parameters of the distribution are estimated from the 2D slice.

Next, prior probabilities are constructed. In,[4] it is suggested that good results can be achieved by setting the priors of the current slice to the posteriors of the previous slice. This has a smoothing effect across time and tends to help push through noise which may occur on slices in time.

In the last step of the algorithm, the likelihood and prior probabilities are used to compute the posterior probabilities, $p(C|V)$, via Bayes' Rule. Following the application of Bayes' Rule, each of the N components of the posteriors are independently spatially smoothed using the anisotropic smoother of Olver *et al.*[5] Teo *et al.* showed that such a smoothing of the posteriors results in a more effective noise removal than a smoothing of the original data.[6]

Finally, the segmentation is completed by assuming that each pixel belongs to the class of maximum probability. It is well known that this "Maximum a posteriori test" minimizes the probability of segmentation error. * Using this decision rule, a final segmentation or label-map is constructed from the smoothed posterior probabilities.

2.2. Volumetric Medical Image Classification

Previously, Teo *et al.*[7] presented results of volumetric Bayesian segmentation on brain MRI scans. Their Bayesian segmentation algorithm was used to detect the white/gray matter boundary. Their algorithm is very similar to the algorithm stated above in Section 2.1. However, instead of iterating through the slices, they simply classified the entire volume in one shot. Therefore, they assumed homogeneous priors. Like the algorithm above, they also smoothed the posteriors and applied a MAP decision rule to achieve segmentation.

---

*It is possible for one to assign various subjective costs for different types of segmentation errors and to then generalize this MAP test to minimize the average Bayes risk; however, we do not wish to penalize any type of error in particular, so the MAP test seems appropriate.
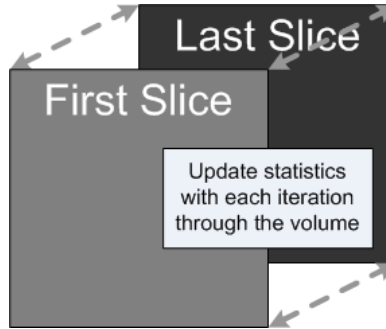
Figure 2. Tissue Tracking General Structure

After applying the Bayesian classification algorithm, Teo *et al.* perform a surface growing morphology operation to grow gray matter uniformly across the white matter surface to a predetermined thickness. They explain the due partial volume effects it is difficult to achieve accurate gray matter segmentations in MRI using this technique.

In other related work, Yang *et al.*[8] developed a Bayesian segmentation algorithm for the segmentation of coronary arteries. In this case, homogeneous priors are also employed. Furthermore, this algorithm works in conjunction with an active contour model to achieve the final result.

2.3. Tissue Tracking

In this subsection, we present the details of our *tissue tracking* algorithm. Specifically, we show how expectation-maximization weights and posterior probabilities may be combined to make intuitive use of the Bayesian priors. Afterwards, we show results of our algorithm on 20 brain MRI data-sets along with validation against expert manual segmentations.

We proceed in a similar fashion as previously introduced in Section 2.1. However, since the data in not time-lapsed, we view the scan axis as the axis of tracking. In Figure 2, we present the basic idea. This algorithm works by iteratively sweeping through the image volume and classifying the volume slice-by-slice. The resulting classification is 3D due to the fact that information is passed between slices through the iterative process.

As in the other algorithms, this algorithm depends upon the user choosing the number, N, of predetermined classes into which the imagery is to be classified. As before, at each step of the iteration through the data-set, our algorithm classifies the given 2D image slice into N classes. The segmentation proceeds as follows, refer to Figure 3 for an overview:

First, the image data is used to generate likelihood probabilities, $p(V|C)$, for a class C and an intensity value V. We assume that the intensities in a given image represent samples from a Gaussian mixture model comprised of N clusters. The parameters for each Gaussian component of the mixture model can be estimated via the expectation-maximization (EM) algorithm. We use the EM algorithm presented by Bilmes *et al.*[9] to estimate the means and variances along with the component weights which provide a measure of the prior probability for each given class.

Next, we construct the prior probabilities, $p(C)$. In many applications, it is difficult to construct meaningful priors by bringing non-data-driven information into the segmentation framework, and thus uniform priors are often employed. We suggest that there are meaningful data-driven priors one may use in these situations. For instance, in[4] the authors reported success using the previous posteriors as the current priors when classifying a time sequence of SAR images. Our method provides a convenient way for one to combine the posteriors from previous medical image slices, call these $p_{POST}(C)$, with the expectation-maximization weights computed from the data, denoted by $p_{EM}(C)$, on the current slice to form the prior probabilities on the current slice.

We begin with an intuitive explanation. For a very small slice spacing, we expect a high degree of correlation from one slice to the next and thus would likely benefit from using the posteriors of the previous slice to guide the
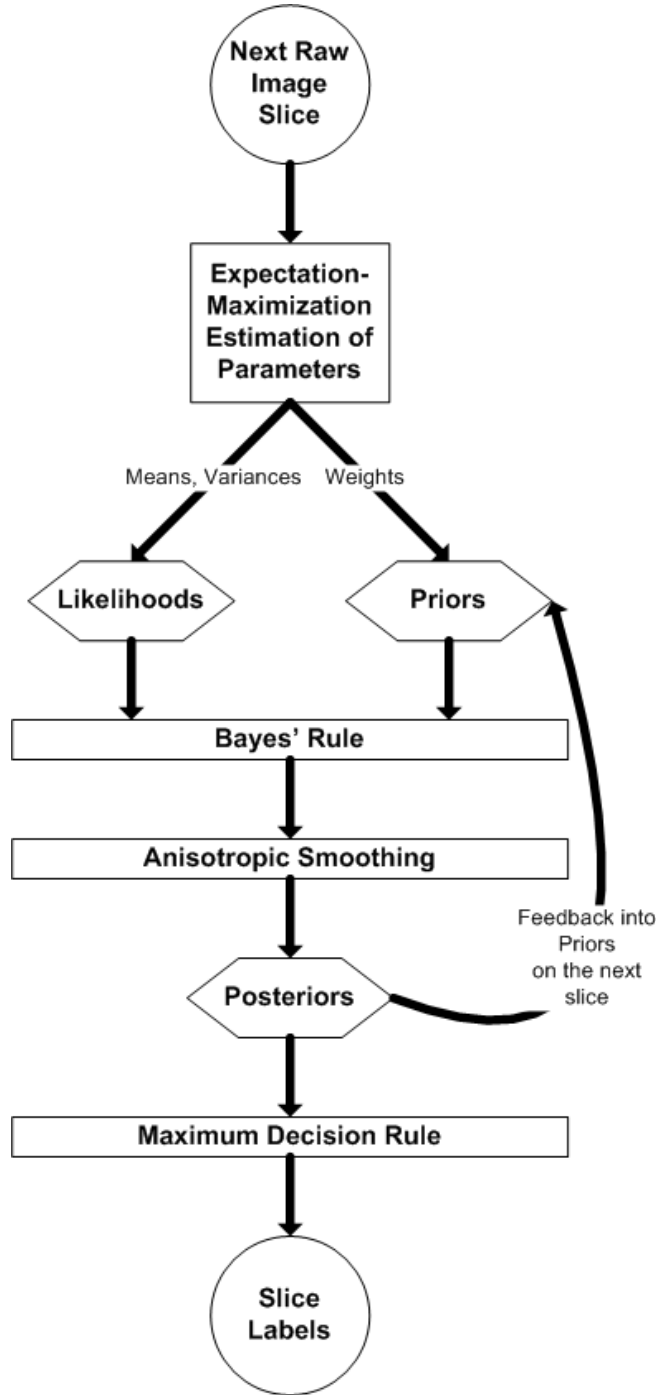
Figure 3. Tissue Tracking Algorithm

choice of priors for the next slice. On the other hand, for a large slice spacing, it is undesirable to use information from previous slices to guide the segmentation of the next slice. In this case, we could set our priors according to the weights derived from the expectation-maximization algorithm. Hence, we use slice spacing, call this Z, to set the contributions of $p_{POST}(C)$ and $p_{EM}(C)$ as follows:

$$p(C) = e^{-Z/\lambda} p_{POST}(C) + (1 - e^{-Z/\lambda}) p_{EM}(C) \qquad (1)$$

where λ is a free parameter which allows the user to tune the weights appropriately.

As before, in the last step of the algorithm, the posterior probabilities are smoothed and the MAP decision rule is applied to achieve the final segmentation.

3. EXPERIMENT

We have applied this algorithm to 20 normal brain MRI data-sets. We used publicly available data-sets from the Internet Brain Segmentation Repository (IBSR) offered by the Massachusetts General Hospital, Center for Morphometric Analysis.[10, 11] The IBSR data-sets are T1-weighted, 3D coronal brain scans after having been positionally normalized. Manual expert segmentations for these data-sets are publicly available and represent the ground truth used in this work.

Also documented on the IBSR website are the details for a comparison of 6 separate classification algorithms on these 20 datasets. They use an overlap metric for validation known as the Tanimoto coefficient[12] which will be discussed further in Section 4. Using the Tanimoto coefficient, Rajapakse *et al.* compared the results of 6 separate algorithms (each operating in the absence of clinical prior information) on the classification of these 20 datasets into gray matter, white matter, and CSF. These 6 algorithms include the following: Adaptive MAP, Biased MAP, Fuzzy C-Means, MAP, Maximum-Likelihood, and Tree-Structure K-Means.

These 20 coronal brain scans are convenient for comparison because they span the spectrum of quality of imagery. The worst cases have low contrast and relatively large intensity gradients. The best cases are more recently acquired and result in better overlap scores.

Our code was written using the Insight Toolkit (ITK).[13] ITK is quickly becoming the imaging software of choice for researchers in the medical imaging community and all of the functionality needed for this algorithm exists in the latest release of ITK (version 3.0.0). In addition to ITK, we relied heavily upon various tools to perform our experiment, such as 3D Slicer[14] and FreeSurfer.[15]

The IBSR data is anisotropic (1mm x 1mm x 3mm), so we set the parameter $Z = 3$. We experimented with a variety of settings for the parameter lambda and found that the best results were achieved by setting $\lambda = 3$. This corresponds to using 36.7% of the neighboring posterior and 63.3% of the EM weights for our prior.

4. RESULTS

Here we compare the results of our algorithm on the 20 IBSR datasets with the 6 algorithms discussed above in Section 3. We validate the results of our algorithm against the expert manual segmentations using the Tanimoto coefficient. The Tanimoto coefficient is defined by $1 - (n_1 + n_2 - 2n_{12})/(n_1 + n_2 - n_{12})$ in which n_1 is the number of voxels of a particular class (e.g. the number of voxel of gray matter) in manual result and n_2 is number of voxels of that same class for the algorithm result. n_{12} represents the number of voxels contained in the intersection of the particular class from manual result and the algorithm result. The metric ranges from 0 to 1 while 1 signifies identical results and 0 indicates poor results. While other popular validation methods exist, such as the DICE measure,[16] the Tanimoto metric represents a good measure of overlap and is convenient for comparing against the IBSR results.

The results of our methods as compared to the 6 other algorithms is shown in Figure 4 for gray matter voxels and in Figure 5 for white matter voxels. As can be seen, our algorithm performs better than the competing algorithms, especially for low quality imagery (note that the cases are ordered from poor quality on the left to high quality on the right).

On average, the tissue tracking algorithm achieves a Tanimoto coefficient of 0.6236 for gray matter compared to 0.5609 for the 3D volumetric version and to 0.5254 for the other methods shown in the plot. Likewise, the tissue tracking algorithm achieves a Tanimoto coefficient of 0.6578 for white matter compared to 0.6039 for the 3D volumetric version and to 0.5580 for the other methods shown in the plot.

In Figures 6, 7, and 8, we show snapshots of our results on various data-sets and slices. In the left column, we show the original grayscale slice. In the middle column, we show the results of our classification algorithm. In the right column, we show the expert manual segmentation results. Note that cases 5-8 and 4-8 were poor quality cases while case 11-3 was a high quality case.
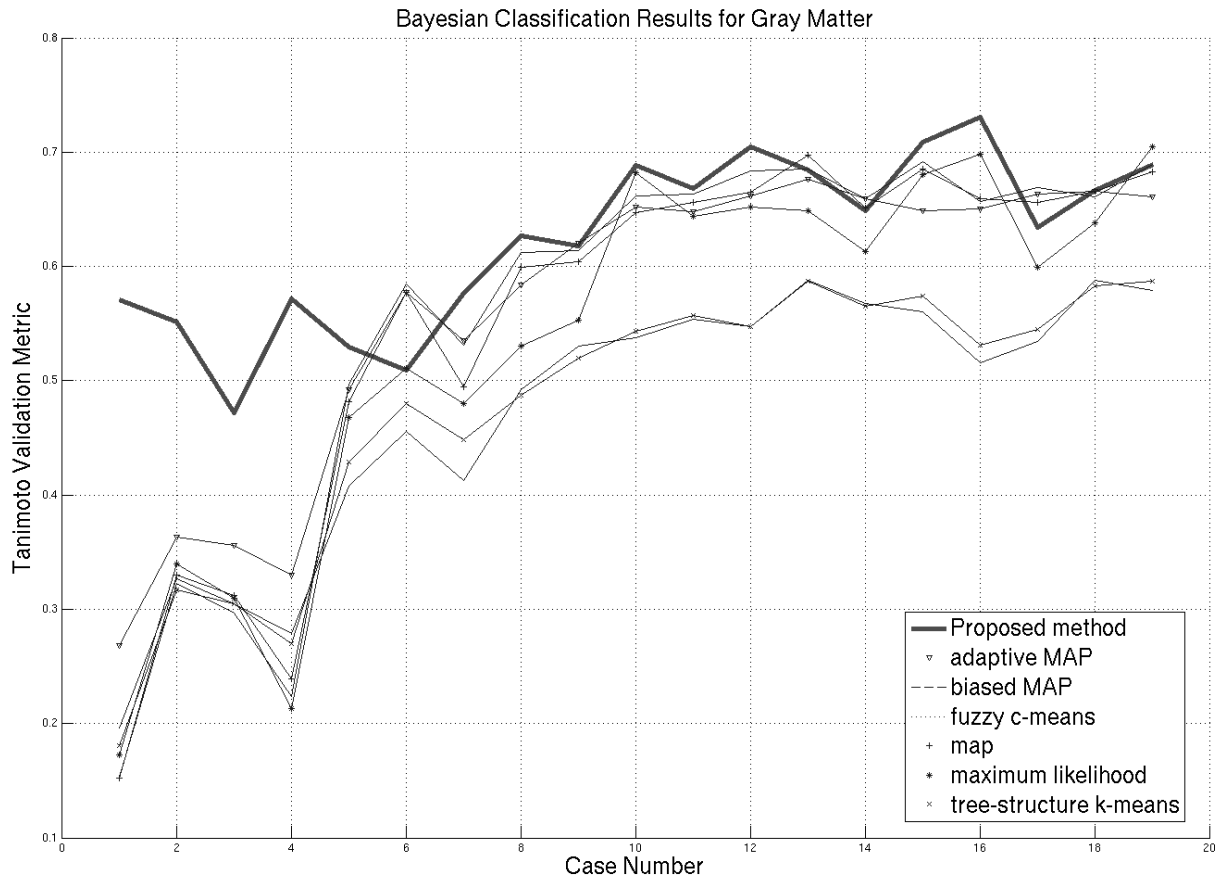
Figure 4. Overlap of Gray Voxels for Each Brain Scan

5. CONCLUSION

We have presented an algorithm for the Bayesian segmentation of imagery by casting the problem in a tracking framework and using priors derived from the data. Using slice thickness, we have proposed a combination of expectation-maximization weighting and previous posterior updating to construct meaningful priors. The application of this algorithm to brain MRI scans has shown positive results.

ACKNOWLEDGMENTS

REFERENCES

1. K. Pohl, J. Fisher, W. Grimson, R. Kikinis, and W. Wells, "A bayesian model for joint segmentation and registration," *NeuroImage* **31**(1), pp. 228–239, 2006.
2. K. Van Leemput, F. Maes, D. Vandermeulen, and P. Suetens, "Automated model-based tissue classification of MR images of thebrain," *Medical Imaging, IEEE Transactions on* **18**(10), pp. 897–908, 1999.
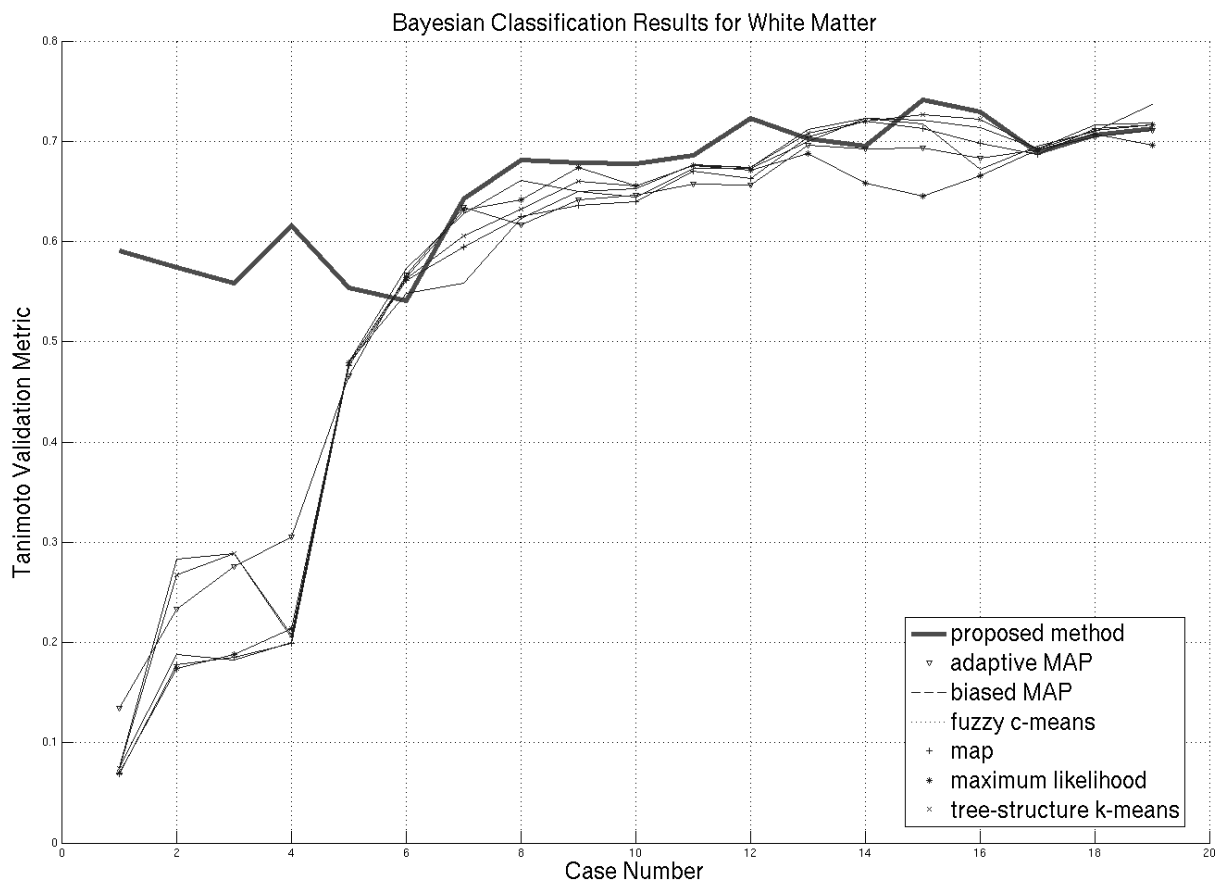
Figure 5. Overlap of White Voxels for Each Brain Scan

3. T. Kapur, "Model based three dimensional Medical Imaging Segmentation," *Massachusetts Institute of Technology* , 1999.

4. S. Haker, G. Sapiro, and A. Tannenbaum, "Knowledge-based segmentation of SAR data with learned priors," *Image Processing, IEEE Transactions on* **9**(2), pp. 299–301, 2000.

5. P. Olver, G. Sapiro, and A. Tannenbaum, "Invariant Geometric Evolutions of Surfaces and Volumetric Smoothing," *SIAM Journal on Applied Mathematics* **57**(1), pp. 176–194, 1997.

6. P. Teo, G. Sapiro, and B. Wandell, "Anisotropic smoothing of posterior probabilities," *Image Processing, 1997. Proceedings., International Conference on* **1**, 1997.

7. P. Teo, G. Sapiro, and B. Wandell, "Creating connected representations of cortical gray matter for functional MRI visualization," *Medical Imaging, IEEE Transactions on* **16**(6), pp. 852–863, 1997.

8. Y. Yang, A. Tannenbaum, and D. Giddens, "Knowledge-based 3D segmentation and reconstruction of coronary arteries using CT images," *Engineering in Medicine and Biology Society, 2004. EMBC 2004. Conference Proceedings. 26th Annual International Conference of the* **1**, 2004.

9. J. Bilmes, "A Gentle Tutorial of the EM Algorithm and its Application to Parameter Estimation for Gaussian Mixture and Hidden Markov Models," *manuscript, International Computer Science Institute* , 1998.

10. C. f. M. A. Massachusetts General Hospital, "Internet brain segmentation repository," 1998. http://www.cma.mgh.harvard.edu/ibsr/.

11. J. Rajapakse and F. Kruggel, "Segmentation of MR images with intensity inhomogeneities," *IMAGE VISION COMPUT* **16**(3), pp. 165–180, 1998.
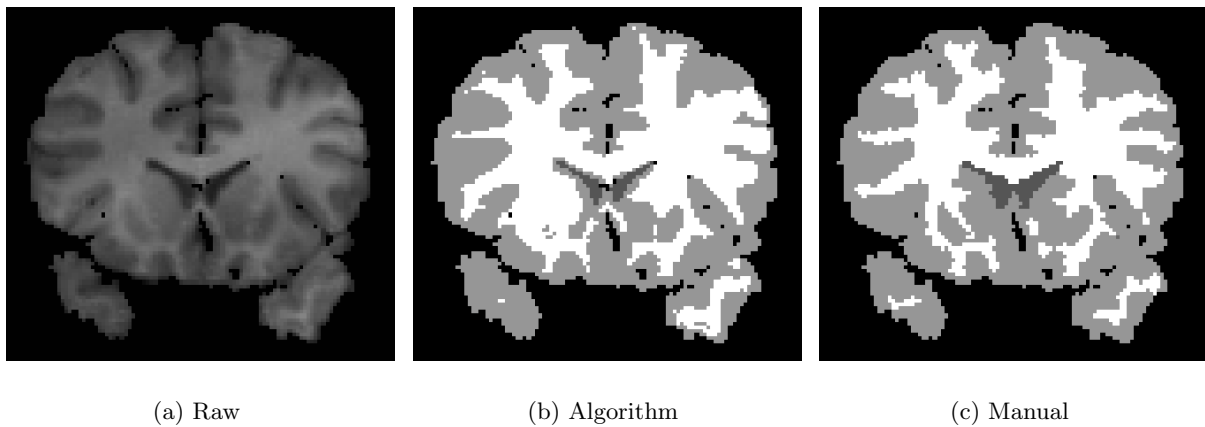
(a) Raw   (b) Algorithm   (c) Manual

Figure 6. Case 5-8, Slice 36

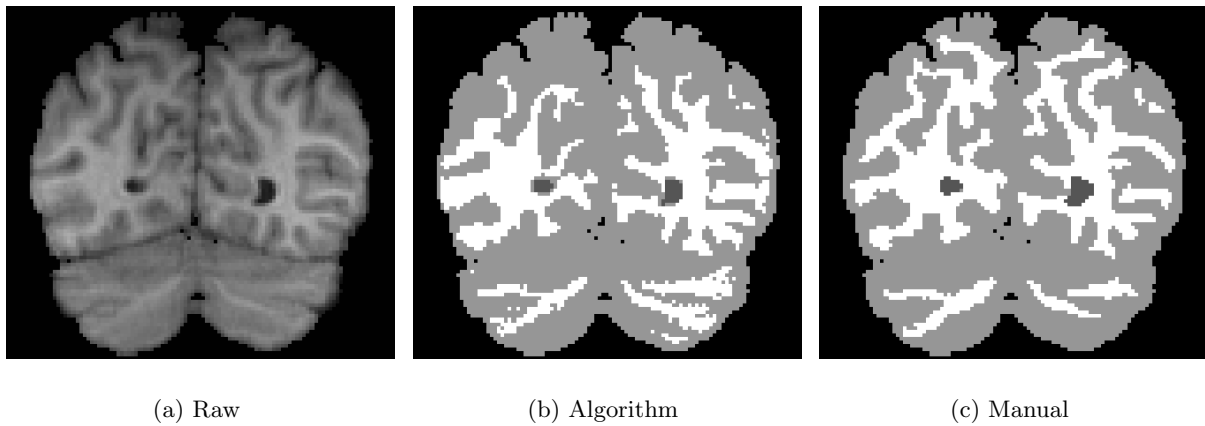(a) Raw   (b) Algorithm   (c) Manual

Figure 7. Case 4-8, Slice 12

12. R. Duda, P. Hart, *et al.*, *Pattern Classification and Scene Analysis*, Wiley New York, 1973.
13. L. Ibanez, W. Schroeder, L. Ng, and J. Cates, "The ITK Software Guide. Kitware, Inc," tech. rep., ISBN 1-930934-10-6, http://www. itk. org/ItkSoftwareGuide. pdf, 2003.
14. D. Gering, A. Nabavi, R. Kikinis, W. Grimson, N. Hata, P. Everett, F. Jolesz, and W. Wells, "An integrated visualization system for surgical planning and guidance using image fusion and interventional imaging," *MICCAI 99: Proceedings of the Second International Conference on Medical Image Computing and Computer Assisted Intervention* , pp. 809–819.
15. F. Segonne, A. Dale, E. Busa, M. Glessner, D. Salat, H. Hahn, and B. Fischl, "A hybrid approach to the skull stripping problem in MRI," *NeuroImage* **22**(3), pp. 1060–1075, 2004.
16. A. Zijdenbos, B. Dawant, R. Margolin, and A. Palmer, "Morphometric analysis of white matter lesions in MR images: method and validation," *Medical Imaging, IEEE Transactions on* **13**(4), pp. 716–724, 1994.

(a) Raw · · · (b) Algorithm · · · (c) Manual

Figure 8. Case 11-2, Slice 44